Received Date : 18-Dec-2016
Accepted Date : 06-Feb-2017
Article type : Communication

Insights into the formation of carlactone from in-depth analysis of the CCD8-catalyzed reactions

Mark Bruno[1], Martina Vermathen[2], Adrian Alder[1], Florian Wüst[1], Patrick Schaub[1], Rob van der Steen[3], Peter Beyer[1], Sandro Ghisla[4*] & Salim Al-Babili[5,1*]

[1]Faculty of Biology, University of Freiburg, D-79104 Freiburg, Germany. [2]Department of Chemistry and Biochemistry, University of Bern, 3012 Bern, Switzerland. [3]Buchem b.v. Biopartner 3, Galileiweg 8, 2333 BD Leiden, the Netherlands. [4]Department of Biology, University of Konstanz, D78457 Konstanz, Germany. [5] King Abdullah University of Science and Technology (KAUST), BESE Division, 23955-6900 Thuwal, Saudi Arabia.

*Corresponding authors:

salim.babili@kaust.edu; sandro.ghisla@uni-konstanz.de

ABSTRACT Strigolactones (SLs) are a new class of phytohormones synthesized from carotenoids via carlactone. The complex structure of carlactone is not easily deducible from its precursor, a *cis*-configured β-carotene cleavage product, and is thus formed via a poorly understood series of reactions and molecular rearrangements, all catalyzed by only one enzyme, the carotenoid cleavage dioxygenase 8 (CCD8). Moreover, the reactions leading to carlactone are expected to form a second, yet unidentified product. In this study, we used ^{13}C and ^{18}O-labelling to shed light on the reactions catalyzed by CCD8. The characterization of the resulting carlactone by LC-MS and NMR, and the identification of the assumed, less accessible second product allowed us to formulate a minimal reaction mechanism for carlactone generation.

Keywords: Apocarotenoid, Carlactone, Carotenoid, Carotenoid cleavage dioxygenase Strigolactone

This article has been accepted for publication and undergone full peer review but has not been through the copyediting, typesetting, pagination and proofreading process, which may lead to differences between this version and the Version of Record. Please cite this article as doi: 10.1002/1873-3468.12593
This article is protected by copyright. All rights reserved.

Accepted Article

1. Introduction

Strigolactones (SLs) are a novel class of phytohormones that shape plant's architecture [1,2,3,4]. In addition, SLs are released into soil where they play a crucial role in establishing the symbiosis of plants with mycorrhizal fungi [5]. However, these compounds also induce seed germination of root parasitic plants of the genus *Striga*, initiating the parasitic attack of these weeds that cause severe yield losses in different crops [6,7]

SLs are carotenoid derivatives, and their biosynthesis (for SLs biosynthesis, see Supplementary Fig. 1) involves the two Carotenoid cleavage dioxygenases CCD7 and CCD8, members of the ubiquitous family of non-heme iron Carotenoid Cleavage Oxygenases (CCOs) [8]. In general, CCOs catalyze the oxidative cleavage of C=C bonds of carotenoids yielding ketone and/or aldehyde product [9]. This leads, *inter alia*, to the formation of physiologically important compounds, like the opsin chromophore retinal and the phytohormone abscisic acid [8,10]. SLs originate from a 9-*cis*-β-carotene that is produced by the carotene isomerase DWARF27 from the corresponding all-*trans*-configured isomer [11,12]. In the next step, CCD7 catalyzes the stereospecific cleavage of 9-*cis*-β-carotene into 9-*cis*-β-apo-10'-carotenal and the volatile β-ionone [11,13]. This reaction is followed by the direct conversion of 9-*cis*-β-apo-10'-carotenal into carlactone via a sequence of complex reactions [11], the mechanisms of which are not yet clear in their details. In rice, carlactone is the substrate of the carlactone oxidase (CO) Os900, a CYP (711 clade), which catalyzes repeated oxygenation and ring closures to form 4-deoxyorobanchol (known as: *ent*-2'-*epi*-5-deoxystrigol), the parent molecule of the orobanchol-like SLs. A second CYP of the same clade, orobanchol (OS, formerly designated as *ent*-2'-*epi*-5-deoxystrigol-4-hydroxylase) converts 4-deoxyorobanchol into orobanchol [14]. In Arabidopsis, MAX1, a CYP (711 clade), converts carlactone into carlactonic acid via the intermediate 19-hydroxy carlactone. Carlactonic acid can be converted into methyl carlactonate [15]. Methyl carlactonate is hydroxylated by LBO (Lateral branching oxidoreductase) into yet unidentified product [16].

The discovery of carlactone [11] (compound **8** in Fig. 1) was a cornerstone in the elucidation of SL biosynthesis, however the steps leading to this compound are still elusive. Moreover, the reactions converting 9-*cis*-β-apo-10'-carotenal (a C_{27} compound) into carlactone (C_{19}) must also concomitantly yield a second product that has not been identified yet. A previously discussed hypothetical mechanism for carlactone formation [11] involves isomerization at positions C_{11} to C_{14} of the chain in the precursor 9-*cis*-β-apo-10'-carotenal (compound **1,** in Fig. 1). It relied on the conclusion by Kloer *et al*. [17] that a related retinal-forming

This article is protected by copyright. All rights reserved.

cyanobacterial enzyme [18] binds substrate and subsequently "… *three consecutive double bonds of this carotenoid changed from a straight all-trans to a cranked cis-trans-cis conformation"* [17]. However, it has been recently shown that this was incorrect [19], the bound molecule representing a polyoxyethylene detergent. A reevaluation of the initial steps of the CCD8 mechanisms was thus one of the aims of the present study along with the following points: we followed the fate of C-chain segments of the substrate (**1**) upon product (**8**) formation using a specific ^{13}C-label. Using $^{18}O_2$ and $H_2{}^{18}O$, we determined the origin of the oxygen atoms in (**8**). Furthermore, we identified the second product (**9**) that results from the cleavage of substrate (**1**) along with (**8**). The results allow the formulating of a minimal mechanism as depicted in Fig. 1.

2. Materials and Methods

2.1. Protein production, enzymatic assays and extraction

CCD7 and CCD8 were produced in *E. coli* and used for the enzymatic production of carlactone as described previously [11]. These protocols also apply for the extraction procedures, the HPLC analysis of carlactone and the estimation of substrate concentrations used.

2.2. Carlactone ^{18}O and ^{13}C-labelling experiments

A micellar suspension of 9-*cis*-β-apo-10'-carotenal, produced enzymatically as described [11], was incubated in the presence of PsCCD8 in a volume scaled up to 2 ml for 3 h at 28 °C in $H_2{}^{16}O$ and bubbled with $^{18}O_2$ (Campro Scientific, Germany). Alternatively, the incubations were conducted in $H_2{}^{18}O$ and in the presence of $^{16}O_2$. For this purpose, the assays were lyophilized, and resuspended in 1 ml $H_2{}^{18}O$ (Campro Scientific, Germany) and incubated for 3 h at 28 °C. For the ^{13}C-labelling of carlactone, 9-*cis*-11-^{13}C-β-apo-10'-carotenal was incubated with PsCCD8 in the presence of the respective micellar suspension of the substrate in a volume scaled up to 2 ml.

2.3. Mass spectrometry

^{18}O-labeled carlactone (**8**; Fig. 1) was analyzed on a Thermo Scientific LTQ Orbitrap XL instrument as described [11]. The identification of ω-OH-(4-CH_3)heptanal (**9**), the second product formed from the incubation of 9-*cis*-β-apo-10'-carotenal with PsCCD8 was achieved after derivatization with penta-fluoro-benzyl-hydroxylamine (PFBHA). A 200 µl

This article is protected by copyright. All rights reserved.

Accepted Article

incubation was stopped after 6 h by adding 200 µl $CHCl_3$:MeOH (2:1, v/v) followed by vortexing and sonication. After centrifugation for 1 min at 17.000 *g*, the organic phase was collected, the extraction repeated and the organic phases combined. 50 µl of an aqueous PFBHA-solution (15 mg/ml) were added to the organic phase and incubated at 35 °C for 2 h of which 5 µl were used for LC-MS analysis with a Q-Exactive mass spectrometer coupled to an UltiMate 3000 UPLC system (Thermo Fisher Scientific). Sample separation was achieved with a Hypersil Gold 1.9 µm C_{18} UPLC-column (150 x 2.1 mm) and the solvent system A, 0.1 vol % formic acid in H_2O and B, 0.1 vol % formic acid in acetonitrile. The flow rate was held constant at 0.5 ml/min for one minute at 70 % B, followed by a gradient to 100 % B within 4 minutes. Final conditions were maintained for 15 min, followed by re-equilibration to initial conditions. Ionization of apocarotenoids was carried out using atmospheric pressure chemical ionization (APCI) in the positive mode. Nitrogen was used as sheath and auxiliary gas, set to 20 and 10 arbitrary units, respectively. The vaporizer temperature was set to 350 °C and the capillary temperature was at 320 °C. The discharge current was set to 5 µA, and normalized collision energy (NCE) to 35 arbitrary units. For data analysis the "TraceFinder 3.1" software was used.

The LC-MS analysis of carlactone and ^{13}C-labeled carlactone was performed using the LC-MS system given above. Sample separation was achieved isocratically at a flow-rate of 0.4 ml/min of 0.1% formic acid in methanol. Ionization of carlactone was carried out using electrospray ionization (ESI) in the positive mode. Nitrogen was used as sheath and auxiliary gas, set to 40 and 15 arbitrary units, respectively. The vaporizer temperature was at 320 °C and the capillary temperature at 300 °C. The discharge current was set to 5 µA and the normalized collision energy (NCE) was set to 40 arbitrary units. The identification of product ions was achieved by collecting data-dependent-MS^2 spectra using $[MH\ Na]^+$ 325.17742 for ^{12}C-carlactone and $[MH\ Na]^+$ 326.18077 for $^{13}C_{11}$-carlactone, respectively as precursor ions.

2.4. NMR analysis

For NMR studies, 800 µg of 9-*cis*-11-^{13}C-β-apo-10'-carotenal (**1**) and 600 µg of purified, biosynthetic carlactone (**8**) were each dissolved in 500 µL CD_2Cl_2. The NMR experiments were done with a Bruker AVANCE III spectrometer operating at a ^{1}H resonance frequency of 400.13 MHz. The instrument is equipped with a 5 mm dual, broad band probe (BBFO Bruker "SmartProbe") with a z-gradient coil and using 90° pulse lengths of 10 µs (^{1}H) and 10 µs (^{13}C). Bruker TOPSPIN software (version 3.2, patch level 3) was used to

This article is protected by copyright. All rights reserved.

Accepted Article

acquire and process the NMR data. The measurements were carried out at room temperature (298 ^{o}K). Simulation of NMR experiments was performed with the Bruker software NMR-Sim (version 5.2.1).

For the 1D ^{1}H experiments, a standard one-pulse experiment (zg) was used, applying 64 transients, a spectral width of 12 ppm, a data size of 32K points, a relaxation delay of 5 s, and an acquisition time of 3.41 s. The free induction decays (FIDs) were exponentially weighted applying a line broadening factor of 0.3 Hz prior to Fourier transformation, phasing and baseline correction.

The 2D ^{1}H-^{13}C-HSQC experiments were carried out applying the gradient-enhanced HSQC experiment with carbon multiplicity editing and echo-antiecho acquisition mode (hsqcedetgpsisp2.2). Eight transients, a relaxation time of 1 s, an acquisition time of 0.21 s, spectral widths of 12 ppm and 220 ppm (in f2 and f1), with 2048 and 128 acquired data points respectively, were used. Data were processed by zero-filling (to 1024) and linear prediction in f1, and by using shifted squared sine window functions in both dimensions prior to Fourier transformation**.**

2.5. Synthesis of 9-cis-11-^{13}C-β-apo-10'-carotenal (I)

The first step of the synthesis is the conversion of commercially available β-ionone (2; Supplementary Fig. 2) into ^{13}C labeled 3-methyl-5-(2,6,6-trimethylcyclohex-1-enyl)penta-2,4-dienenitrile via an *in situ* Horner-Wadsworth-Emmons (HWE) reaction. After deprotonation of 1-^{13}C acetonitrile with one equivalent of lithium diisopropylamide (LDA), the anion formed was reacted with diethyl chlorophosphate to give ^{13}C labeled diethyl cyanomethylphosphonate, which was immediately deprotonated by a second equivalent of LDA [20]. The nitrile obtained as a mixture of 2-*trans* and *2-cis* isomers, was reduced with dibal-H to yield ^{13}C labeled 3-methyl-5-(2,6,6-trimethyl-cyclohex-1-enyl)penta-2,4-dienal. The 2-*trans* and 2-*cis* isomers were separated by column chromatography to afford the pure 2-*cis* isomer (3) used in the next step. (3) Was reacted with diethyl(3-cyano-2-methyl-2-propenyl)phosphonate in a HWE reaction with NaH as base. The phosphonate synthon was prepared in two steps from chloroacetone, diethylcyanomethylphosphonate and NaH as base, followed by an Arbusov reaction with triethylphosphite [21,22]. The nitrile obtained as a mixture of 2-*trans*, 4-*trans*, 6-*cis* and 2-*cis*, 4-*trans*, 6-*cis* isomers was reduced with dibal-H to the ^{13}C labeled 3,7-dimethyl-9-(2,6,6-trimethylcyclohex-1-enyl)nona-2,4,6,8-tetraenal. The 2-*trans*, 4-*trans*, 6-*cis* and 2-*cis*, 4-*trans* , 6-*cis* isomers were separated by column chromatography to provide the pure 2-*trans*, 4-*trans*, 6-*cis* isomer (4) used in the next step. The pure 2-*trans*, 4-*trans*, 6-*trans*, 8-*trans*, 10-*cis* isomer of 2,7,11-trimethyl-13-(2,6,6-

This article is protected by copyright. All rights reserved.

Accepted Article

trimethylcyclohex-1-enyl)trideca-2,4,6,8,10,12-hexaenal (5) was obtained via a similar two step strategy and the purification method described for the conversion of (3) to (4), but instead of diethyl(3-cyano-2-methyl-2-propenyl)phosphonate, the slightly different diethyl(3-cyano-3-methyl-2-propenyl)phosphonate was used. This phosphonate synthon was first prepared in a three step sequence [23]. Propionitrile was deprotonated with one equivalent of n-butyllithium at -60 ^{o}C to form the α-anion that was directly reacted *in situ* with diethylchlorophosphate to form diethyl-1-cyanoethylphosphonate. The latter was again deprotonated with a second equivalent of n-butyllithium followed by addition of chloroacetaldehyde. A subsequent Arbuzov reaction with triethylphosphite resulted in the synthon mentioned above. Finally the pure ^{13}C labeled 2-*trans*, 4-*trans*, 6-*trans*, 8-*trans*, 10-*trans*, 12-*cis* isomer (1) was obtained by a standard HWE elongation with diethylcyanomethyl-phosphonate and NaH followed by a dibal-H reduction and subsequent silica gel purification and crystallization. A scheme for the synthesis is shown in Supplementary Fig. 2.

The ^{13}C enrichment of (1) is confirmed by comparison of the 1D ^{1}H- and 2D ^{1}H-^{13}C-HSQC NMR spectra of labeled (1*) and unlabeled (1) (Supplementary Fig. 3-8). (1*) exhibits an intense cross peak in the ^{1}H-^{13}C-HSQC spectrum at 6.92 ppm/125.9 ppm with a triplet structure in the proton dimension (Supplementary Fig. 8) matching the assignment of 11-CH in (1).

3. Results and Discussion

Whether CCOs are mono-or dioxygenases remains debated, however, evidence in favor of the latter is mounting [24]. To determine which of the two mechanisms is utilized by CCD8, we incubated 9-*cis*-β-carotene with *Pisum sativum* PsCCD7 and PsCCD8 in presence of $^{18}O_2/H_2{}^{16}O$. The obtained carlactone (**8**) has a $[M+H]^+$ of 309.2081 (Fig. 2 a), compatible with the incorporation of three ^{18}O atoms. The companion experiment carried out in the presence of $^{16}O_2$ and $H_2{}^{18}O$ yielded (**8**) with a $[M+H]^+$ of 303.1952, i.e. smaller by 6 atom units. Incubation of (**1**) with PsCCD8 in the presence of $^{18}O_2$ and $H_2{}^{16}O$ also led to triple ^{18}O-labeling of (**8**). This shows that none of the O atoms in (**8**) derive from the aldehyde group of the precursor (**1**) and is fully compatible with CCD8 acting as a dioxygenase in generating carlactone.

This article is protected by copyright. All rights reserved.

Accepted Article

The structure of carlactone (**8**) elucidated previously reveals a truncation by 8 C-atoms relative to the educt [11]. For the formulation of a reaction mechanism, the fate of this chain fragment of (**1**), i.e. the identification of the second product, is mandatory. Original attempts to find the presumed ampholytic C_8 moiety (**9**) failed, likely due to its instability/reactivity. Therefore, we used in the present work the ketone/aldehyde selective derivatization reagent pentafluoro-benzyl-hydroxylamine (PFBHA) that enabled us to detect a compound with $[M+H]^+ = 334.0861$ corresponding to the formula $C_{15}H_{13}O_2NF_5$ (Fig. 2 c). This is the product expected from derivatization of (**9**), thus confirming its structure.

To identify the segment that yields the lactone moiety of carlactone (**8**), we synthesized (**1**) with a ^{13}C label at C_{11} (C_{11} corresponds to the C_2' atom in the SLs numbering convention, see Supplementary Fig. 1; ^{13}C labelled compounds are denoted with (*); for the chemical synthesis of ^{13}C-labelled (**1**), see Supplementary Fig. 2). The ^{13}C enrichment of (**1***) was confirmed by the NMR spectra presented and discussed in the Supplementary Data (Supplementary Fig. 3-8). The MS^2 spectrum of (**8***) produced from (**1***) using *Arabidopsis thaliana* (At) CCD8 is compatible with the presence of one ^{13}C in the butenolide ring of (**8***) (Fig. 2 b, and Fig. 1). This assignment is confirmed by the comparison of the ^1H and ^{13}C NMR spectra of (**8***) with those previously reported for unlabeled carlactone [11] (**8**) shown in Fig. 3 (see also Supplementary Fig. 9-13). Essentially complete incorporation of the ^{13}C-label at C_{11} in (**8***) is deduced from the NMR spectra of Fig. 3.

The formulation of a biochemical mechanism as in Fig. 1 bases on the following observations: *(i)* CCD8 utilizes 9-*cis*-β-apo-10'-carotenal (**I**) and O_2 as the sole substrates for the synthesis of (**8**). *(ii)* Carlactone (**8**) and ω-OH-(4-CH_3)heptanal (**9**) are the only two products formed. *(iii)* Two bonds (C_{10}-C_{11}, and C_{14}-C_{15}) of the carotenal chain (**1**) are cleaved during the process. The three oxygen atoms present in (**8**) derive from O_2 and not from H_2O or the aldehyde function of (**1**), as shown by $^{18}O_2$ and $H_2{}^{18}O$ labeling experiments. Thus, (*iv),* two equivalents of O_2 are consumed in the overall process. *(v)* This is compatible with the occurrence of a dioxygenase reaction [25] that takes place twice. *(vi)* The $^{13}C_{11}$ label of (**1**) is found at the C_{11} "diol" bridge position in the butenolide moiety of (**8**). *(vii)* The *cis* (or ring) configuration of the C_{12}-C_{13} double bond in (**8**) requires the *transoid* configuration at C_{12}-C_{13} in the educt (**I**) to be converted into a *cisoid* one along the path leading to (**8**). *(viii)* The chemical transformations ought to result in a *R*-configuration at C_{11} of (**8**) [10]. Finally, *(ix)* CCD8 works on carotenal substrates that are configured either *cis* or *trans* at C_9=C_{10}. When *trans* configured, the reaction yields the canonical CCD single cleavage products β-apo-13-carotenone and a C_9-dialdehyde [11,26], supposedly via a dioxygenase reaction [9].

This article is protected by copyright. All rights reserved.

Accepted Article

The argument outlined under *(vii)* states that the *transoid* configuration at C_{12}-C_{13} in (**1**) must be converted into a *cisoid* one (see (a), (**2**) Fig. 1). This involves a simple rotation of the substituents around the C_{12}-C_{13} bond. Rowan *et al.* [27] have estimated the barrier for this rotation for the closely related 11-*cis*-retinal from NMR data. They conclude that it is relatively low and state that … *when bound to the protein opsin to form rhodopsin, retinal could have either conformation about the 12-13 bond."* A similar conclusion is reached by a recent theoretical work [28]. The standard CCD cleavage reaction mechanism [9,29-32] is supposed to proceed through a dioxetane-involving variant as the more likely route [33]. This correlates with theoretical calculations of dioxygenase reaction profiles [31]. Taking into account that CCD8 is capable of catalyzing a standard single cleavage reaction with the all-*trans* configured substrate (see *ix*), it appears reasonable to assume that the same catalytic machinery is also used with the C_9=C_{10}-*cis* substrate (**1**), i.e. the "dioxetane variant". Since chain cleavage occurs at bonds involving C_{14} with both the *trans*- and the *cis*-substrate [25], it appears likely that the initial event in both oxygenations involves an attack by the presumed Fe^{III}-O-O$^{\cdot}$ species at C_{14}. In other words, with the C_9=C_{10}-*cis* substrate the attack is at C_{14} + C_{11} to form the cyclic endo-peroxide (**4**), while with the *trans* substrate it is at C_{14} + C_{13} to form a C_{13}-C_{14} cyclic peroxide [9]. Thus, the selection of the second position of attack in addition to C_{14} (C_{11} or C_{13}) to form the peroxide is likely determined by the *cis* or *trans* configurations at C_9=C_{10} of the respective substrate. With (**2**) the resulting cyclic (endo-) peroxide (**4**) formed via step (b), Fig. 1, would be reminiscent of similar ones found within the cyclooxygenase family [34]. The second oxygenation step (e) to form (**4**) [25] would also occur at the same C_{14}-C_{11} centers. The formation of the peroxides might proceed via single electron transfer steps [25,34,35].

The key events in the overall process are the oxidative chain cleavages involving bond migrations that are represented by steps (d) and (f) in Fig. 1. These can be described as a variant of the well-known Baeyer-Villiger reaction [36,37] and might proceed via Criegee intermediates [37]. The first rearrangement would be initiated by abstraction of the (acidic) C_{14}-H in (**3**) (step (c)) by an active center base such as with a pK_a 6-8 as inferred by Harrison *et al*. [38]. Interaction of the peroxide with the $Fe^{2/3+}$-center or an acid catalyst would assist the reaction, which involves migration of the C_{10}-C_{11} bond. The second Baeyer-Villiger type step (f) would proceed analogously and involve migration of the C_{14}-C_{15} bond. Formation of the final product carlactone (**8**) requires formation of the butenolide ring by a transesterification reaction at the stage of (**7**), step (g).

This article is protected by copyright. All rights reserved.

Accepted Article

The driving force for the formation of the lactone ring of (**8**) is assumed to be due to the expulsion of (**9**), an extensively conjugated ω-OH-aldehyde that should be a good leaving group. This species should be quite a strong acid with a $pK_a \approx 4$ [39], which compares to an estimated pK_a >12 for the postulated, geminal alcoholate (**7**). The corresponding $\Delta pK \geq 8$ would yield a "driving force" of >10 Kcal for the ring closure reaction. It should also be noted that CCD8 catalysis of the "*cis*-reaction" (with respect to C_9=C_{10}, i.e. with (**1**)) is ≈10-fold faster than the reaction with the C_9=C_{10} "*trans*-substrate" [11]. This suggests that the machinery of CCD8 is set-up for dioxygenase and Baeyer-Villiger type catalysis, the second being the preferred one and effective only for C_9=C_{10} "*cis*-substrates", presumably for steric reasons.

Finally, we would like to emphasize that the reaction scheme presented in Fig. 1 should be viewed as a minimal hypothesis. Variants involving different sequences of some steps or proceeding via radical intermediates and adducts are conceivable, but cannot be addressed in the present context.

Acknowledgments

We thank Dr. S. Schürch (University of Bern, Switzerland) for the MS-spectra of ^{18}O-labeled carlactone, and Prof. Dr. A Bacher, (TU München, Germany) for most helpful comments. Research reported in this publication was supported by the King Abdullah University of Science and Technology (KAUST).

References

[1] Al-Babili, S., and Bouwmeester, H. J. (2015) Strigolactones, a Novel Carotenoid-Derived Plant Hormone. Annu. Rev. Plant Biol. 66, 161–186.

[2] Brewer, P.B., Koltai, H., and Beveridge, C.A. (2013) Diverse roles of strigolactones in plant development. Mol. Plant. 6, 18-28.

[3] Seto, Y., and Yamaguchi, S. Strigolactone biosynthesis and perception. (2014) Curr. Opin. Plant Biol. 21, 1-6.

[4] Waldie, T., McCulloch, H., and Leyser, O. (2014) Strigolactones and the control of plant development: lessons from shoot branching. Plant J. 79, 607-22.

[5] de Saint Germain, A., Bonhomme, S., Boyer, F.D., and Rameau, C. (2013) Novel insights into strigolactone distribution and signalling. Curr. Opin. Plant Biol. 16, 583-9.

[6] Akiyama, K., Matsuzaki, K., and Hayashi, H. (2005) Plant sesquiterpenes induce hyphal branching in arbuscular mycorrhizal fungi. Nature 435, 824–7.

This article is protected by copyright. All rights reserved.

Accepted Article

[7] Xie, X., Yoneyama, K., and Yoneyama, K. (2010) The strigolactone story. Annual Review of Phytopathology 48, 93–117.

[8] Ruyter-Spira, C., Al-Babili, S., van der Krol, S., and Bouwmeester, H. (2013) The biology of strigolactones. Trends Plant Sci. 18, 72-83.

[9] Giuliano, G., Al-Babili, S., von Lintig, J. (2003) Carotenoid oxygenases: cleave it or leave it. Trends in Plant Science 8, 145–149.

[9] Kloer, D. P., and Schulz, G. E. (2006) Structural and biological aspects of carotenoid cleavage. Cell. Mol. Life Sci. 63, 2291–303.

[10] Walter, M. H., and Strack, D. (2011) Carotenoids and their cleavage products: biosynthesis and functions. Nat. Prod. Rep. 28, 663–92.

[11] Alder, A., Jamil, M., Marzorati, M., Bruno, M., Vermathen, M., Bigler, P., Ghisla, S., Bouwmeester, H., Beyer, P., and Al-Babili, S. (2012) The Path from β-Carotene to Carlactone, a Strigolactone-Like Plant Hormone. Science. 335, 1348–1351.

[12] Bruno, M., and Al-Babili, S. (2016) On the substrate specificity of the rice strigolactone biosynthesis enzyme DWARF27. Planta 243, 1429–1440.

[13] Bruno, M., Hofmann, M., Vermathen, M., Alder, A., Beyer, P., and Al-Babili, S. 2014. On the substrate- and stereospecificity of the plant carotenoid cleavage dioxygenase 7. FEBS Letters 588: 1802–1807.

[14] Zhang, Y., van Dijk, A. D. J., Scaffidi, A., Flematti, G. R., Hofmann, M., Charnikhova, T., Verstappen, F., Hepworth, J., van der Krol, S., Leyser, O., Smith, S. M., Zwanenburg, B., Al-Babili, S., Ruyter-Spira, C., and Bouwmeester, H. J. (2014) Rice cytochrome P450 MAX1 homologs catalyze distinct steps in strigolactone biosynthesis. Nat. Chem. Biol. 10, 1028–1033.

[15] Abe, S., Sado, A., Tanaka, K., Kisugi, T., Asami, K., Ota, S., Kim, H. Il, Yoneyama, K., Xie, X., Ohnishi, T., Seto, Y., Yamaguchi, S., Akiyama, K., Yoneyama, K., and Nomura, T. (2014) Carlactone is converted to carlactonoic acid by MAX1 in Arabidopsis and its methyl ester can directly interact with AtD14 in vitro. Proc. Natl. Acad. Sci. 111, 18084–18089.

[16] Brewer, P.B., Yoneyama, K., Filardo, F., Meyers, E., Scaffidi, A., Frickey, T., Akiyama, K., Seto., Y., Dun, E.A., Cremer, J.E., Kerr, S.C., Waters, M.T., Flematti, G.R., Mason, M.G., Weiller, G., Yamaguchi, S., Nomura, T., Smith, S.M., Yoneyama, K., Beveridge, C.A. (2016) LATERAL BRANCHING OXIDOREDUCTASE acts in the final stages of strigolactone biosynthesis in Arabidopsis. Proc. Natl. Acad. Sci. 113, 6301–6306.

[17] Kloer, D. P., Ruch, S., Al-Babili, S., Beyer, P., and Schulz, G. E. (2005) The Structure of a Retinal-Forming Carotenoid Oxygenase. Science 308, 267–269.

[18] Ruch, S., Beyer, P., Ernst, H., and Al-Babili, S. (2005) Retinal biosynthesis in Eubacteria: in vitro characterization of a novel carotenoid oxygenase from Synechocystis sp. PCC 6803.Mol. Microbiol. 4, 1015-24.

This article is protected by copyright. All rights reserved.

Accepted Article

Accepted Article

[19] Sui, X., Kiser, P. D., Che, T., Carey, P. R., Golczak, M., Shi, W., Von Lintig, J., and Palczewski, K. (2014) Analysis of carotenoid isomerase activity in a prototypical carotenoid cleavage enzyme, apocarotenoid oxygenase (ACO). J. Biol. Chem. 289, 12286–99.

[20] Creemers, A. F. L., and Lugtenburg, J. (2002) The preparation of all-*trans* uniformly (13)C-labeled retinal via a modular total organic synthetic strategy. Emerging central contribution of organic synthesis toward the structure and function study with atomic resolution in protein research. J. Am. Chem. Soc. 124, 6324–34.

[21] Fujiwara Kazuyoshi, TakahashiHidetaka, and OhtaMasaki. (1962) 4-Chloro-3-methylcrotonic Acid Derivatives and Phosphonates. Bull. Chem. Soc. Jpn. 35, 1743–1744.

[22] Pardoen, J. A., Mulder, P. P. J., Berg, E. M. M. van den, and Lugtenburg, J. (1985) Synthesis of 8-, 9-, 12-, and 13-mono- 13 C-retinal. Can. J. Chem. 63, 1431–1435.

[23] Gebhard, R., van der Hoef, K., Lefeber, A. W. M., Erkelens, C., and Lugtenburg, J. (1990) Synthesis and spectroscopy of (14′-13C)- and (15′-13C)spheroidene. Recl. des Trav. Chim. des Pays-Bas 109, 378–387.

[24] Sui, X., Golczak, M., Zhang, J., Kleinberg, K. A., von Lintig, J., Palczewski, K., and Kiser, P. D. (2015) Utilization of Dioxygen by Carotenoid Cleavage Oxygenases. J. Biol. Chem. 290, 30212–23.

[25] Smith, W. L., Garavito, R. M., and DeWitt, D. L. (1996) Prostaglandin Endoperoxide H Synthases (Cyclooxygenases)-1 and -2. J. Biol. Chem. 271, 33157–33160.

[26] Alder, A., Holdermann, I., Beyer, P., and Al-Babili, S. (2008) Carotenoid oxygenases involved in plant branching catalyse a highly specific conserved apocarotenoid cleavage reaction. Biochem. J. 416, 289–96.

[27] III, R. R., Warshel, A., Skyes, B. D., and Karplus, M. (1974) Conformation of retinal isomers. Biochemistry 13, 970–981.

[28] Bondar, A.-N., Knapp-Mohammady, M., Suhai, S., Fischer, S., and Smith, J. C. (2011) Ground-state properties of the retinal molecule: from quantum mechanical to classical mechanical computations of retinal proteins. Theor. Chem. Acc. 130, 1169–1183.

[29] Harrison, P. J., and Bugg, T. D. H. (2014) Enzymology of the Carotenoid Cleavage Dioxygenases: Reaction Mechanisms, Inhibition & Biochemical Roles. Arch. Biochem. Biophys. 544, 105–11.

[30] Bugg, T. D., and Ramaswamy, S. (2008) Non-heme iron-dependent dioxygenases: unravelling catalytic mechanisms for complex enzymatic oxidations. Curr. Opin. Chem. Biol. 12, 134–140.

[31] Borowski, T., Blomberg, M. R. a, and Siegbahn, P. E. M. (2008) Reaction mechanism of apocarotenoid oxygenase (ACO): a DFT study. Chemistry 14, 2264–76.

[32] Vogel, J. T., Tan, B., Mccarty, D. R., and Klee, H. J. (2008) The carotenoid cleavage dioxygenase 1 enzyme has broad substrate specificity, cleaving multiple carotenoids at two different bond positions. J. Biol. Chem. 283, 11364–73.

This article is protected by copyright. All rights reserved.

[33] Sui, X., Kiser, P. D., Lintig, J. von, and Palczewski, K. (2013) Structural basis of carotenoid cleavage: from bacteria to mammals. Arch. Biochem. Biophys. 539, 203–213.
[34] van der Donk, W. A., Ah-Lim Tsai, A., and Kulmacz, R. J. (2002) The Cyclooxygenase Reaction Mechanism. Biochemistry 41, 15451–8.
[35] Bugg, T. D. H. (2003) Dioxygenase enzymes: catalytic mechanisms and chemical models. Tetrahedron 59, 7075–7101.
[36] Torres Pazmiño, D. E., Dudek, H. M., and Fraaije, M. W. (2010) Baeyer–Villiger monooxygenases: recent advances and future challenges. Curr. Opin. Chem. Biol. 14, 138–144.
[37] Polyak, I., Reetz, M. T., and Thiel, W. (2012) Quantum Mechanical/Molecular Mechanical Study on the Mechanism of the Enzymatic Baeyer–Villiger Reaction. J. Am. Chem. Soc. 134, 2732–2741.
[38] Harrison, P. J., Newgas, S. A., Descombes, F., Shepherd, S. A., Thompson, A. J., and Bugg, T. D. H. (2015) Biochemical Characterisation & Selective Inhibition of β-Carotene cis-trans-Isomerase D27 and Carotenoid Cleavage Dioxygenase CCD8 on the Strigolactone Biosynthetic Pathway. FEBS J. 282, 3986–4000.
[39] Moschel, R. C., and Leonard, N. J. (1976) Fluorescent modification of guanine. Reaction with substituted malondialdehydes. J. Org. Chem. 41, 294–300.

Figure 1. Proposed mechanism of 9-*cis*-β-apo-10´-carotenal (I) conversion into carlactone (8). Roman numerals in blue denote various species and intermediates; letters in black denote minimal steps. R_1 stands for a residue corresponding to the C skeleton of β-ionone, R_2 for the 5 carbon chain C_{17}-C_{21} of (**1**), ~B| for an active center base, and Fe^{n+} for an active center Fe ion. Oxygen(s) in red represent atoms/molecules that are inserted at the indicated positions in the product (**8**) based on experiments using $^{18}O_2$. Bonds in magenta are those that undergo *transoid-cisoid* isomerization in (I) by rotation around the C_{12}-C_{13} bond in step (a). Bonds in green must undergo cleavage for the formation of 8 and migrate to oxygen atoms in steps (d) and (f). These migrations are assumed to occur by mechanisms analogous to the Baeyer-Villiger/Criegee ones [4, 31-37]. Blue circles represent the positions (at C_{11}) of the ^{13}C-label in the educt 1 and as found in the product (**8**); note the C_{11}-R steric configuration of the latter. The stereochemistry of the reactions has been formulated such as to lead to a C_{11}-*R*-configuration in (**8**). Thus, and in the 2D representation of the Figure, reactions with the presumed Fe^{III}-O-O• species (steps (b) and (e)) are depicted arbitrarily as occurring from below the paper plane. This bases on the assumption that the reciprocal orientation of active center functionalities and substrate derived species is similar (conserved) for the two, subsequent dioxygenation steps (b) and (e). Note that the $C_{11/12}$ to C_{21} double bonds in (**4**) and

This article is protected by copyright. All rights reserved.

Accepted Article

(**5**) are in a coplanar configuration, the corresponding part of species (**5**) being planar. The delocalization of the formed negative charge in (**4**) contributes to the "acidification" of the C_{14}-H that is assumed to be abstracted by an active center base ~B| in step (c). This is the prerequisite for the following rearrangement represented by step (d). (**9**) represents mesomeric forms of the secondary product that contribute to the stabilization of its negative charge (estimated $pK_a \approx 4$) [37]. The 3D representations of the structures (**1**) to (**9**) can help visualizing the structural conversions, and are to be found in the Supplementary Fig. 15. Note that inverted sequences of oxygenation ((b) and (e)) and rearrangement steps ((d) and (f)) would lead to a product lactone (analogous to **8**) linked to a molecule fragment derived from R_2; this is illustrated in Supplementary Fig. 16.

Figure 2. ^{18}O and ^{13}C incorporation into carlactone (**8**) and identification of ω-OH-(4-CH_3)-hepta-2,4,6-trien-al (**9**). (a): Quasimolecular ions ([M+H^+]) of unlabeled (upper panel) and triple ^{18}O-labeled carlactone (**8**) (lower panel) obtained by incubations in $^{16}O_2$ / $H_2{}^{18}O$ or $^{18}O_2$ / $H_2{}^{16}O$, respectively. (b): MS^2 spectra of unlabeled (upper panel) and ^{13}C-labeled carlactone (8) (lower panel). Note the mass gain in the butenolide fragment resulting from the ^{13}C atom at position C_{11}. Na-adducts were formed to about 95% under the condition used. c): LC-MS identification of the secondary product (**9**). Lower panel: LC-MS profile of an extract from an incubation of (1) with CCD8 upon derivatization with PFBHA. The target mass represents the $[M+H]^+$ of the ω-OH-(4-CH_3)heptanal PFBHA adduct shown in the inset. The compound is absent in control incubations lacking CCD8 (upper panel).

Figure 3. Comparison of 1D ^1H-NMR spectra of (a) unlabelled (**8**) versus (b) labelled carlactone (**8***) and (C) 2D ^1H-^{13}C-HSQC spectrum of (**8***). The top traces show expansions of the 1D ^1H-NMR spectra of (**8**) (A, in blue) and of (**8***) (B, in black) with resonance assignments. In the ^1H spectrum of (**8***) the resonance of 11-C*H is split into a doublet due to its one bond coupling to the ^{13}C enriched 11-C with a typically large coupling constant of $^1J_{CH}$ = 180 Hz. This indicates essentially complete incorporation of the ^{13}C-label at 11-C. The main panel (C) shows an expansion of the 2D ^1H-^{13}C-HSQC spectrum of (**8***) with cross peaks from ^{13}C-^1H-one-bond ($^1J_{CH}$) couplings between protons and carbons of (**8***). An intense cross peak was observed at 5.97 ppm/100.7 ppm, which was assigned to 11-C*H based on the shifts previously reported for (**8**) [11]. Due to ^{13}C decoupling performed in the HSQC experiment the cross peak appears as a singlet in the ^1H domain corresponding to the central shift position of the large doublet shown in (b). The intensity of this cross peak was much higher than the intensity of the remaining cross peaks deriving from natural abundance

This article is protected by copyright. All rights reserved.

Accepted Article

^{13}C nuclei of (**8***). To display these peaks simultaneously, the lower part of the 2D HSQC spectrum was scaled up by a factor of x64. This high intensity gain of 11-C*H is a further proof of the selective ^{13}C enrichment at position 11-C in (**8***). For full range spectra, see Supplementary Figures.

Supplementary Figure 1. SLs structures and biosynthesis. Canonical SLs, such as orobanchol, consist of a tricyclic lactone (ABC ring) that is connected to a further cyclic lactone (D-ring) by an enol ether bridge. The numbering of C atoms is shown exemplarily for orobanchol. Canonical SLs are divided into the strigol- and orobanchol-like subfamilies, which differ in the stereochemistry of the C8b/C3a atoms (shown in the orobanchol structure). SLs biosynthesis starts with the reversible 9-*cis*/all-*trans* isomerization of β-carotene catalyzed by DWARF27 to yield 9-*cis*-β-carotene. CCD7 then cleaves the latter at the C9'-C10' double bond in the *trans*-moiety of the substrate, to yield 9-*cis*-β-apo-10'-carotenal and β-ionone. The central enzyme is CCD8 that converts the shaded part of 9-*cis*-β-apo-10'-carotenal into carlactone [1] (**s. Fig. 1** and **2**). In rice, carlactone is the substrate of the carlactone oxidase (CO) Os900, a CYP (711 clade), which catalyzes repeated oxygenation and ring closures to form 4-deoxyorobanchol (known as: *ent*-2'-*epi*-5-deoxystrigol), the parent molecule of the orobanchol-like SLs. A second CYP of the same clade, orobanchol synthase (OS, formerly designated as *ent*-2'-*epi*-5-deoxystrigol-4-hydroxylase) converts 4-deoxyorobanchol into orobanchol [2]. In Arabidopsis, MAX1, a CYP (711 clade), converts carlactone into carlactonic acid via the intermediate 19-hydroxy carlactone. Carlactonic acid can be converted into methyl carlactonate [3] and further hydroxylated by the Lateral branching oxidoreductase into a yet unidentified product [4]. In rice, carlactonic acid is likely a further precursor of 4-deoxyorobanchol. 5-Deoxystrigol, the parent of the strigol-like SLs is supposedly formed from carlactone by yet unidentified CYPs.

Supplementary Figure 2. Chemical synthesis of 9-*cis*-11-^{13}C-β-apo-10'-carotenal (I).
(a). LDA (2 eq.), Diethylchlorophosphate, $CH_3{}^{13}CN$, THF, -60 ^{o}C;
(b). Dibal-H, separation isomers;
(c). Diethyl(3-cyano-2-methyl-2-propenyl)phosphonate, NaH/THF;
(d). Dibal-H, separation isomers;
(e). Diethyl(3-cyano-3-methyl-2-propenyl)phosphonate, NaH/THF;
(f). Dibal-H, separation isomers;
(g). Diethylcyanomethylphosphonate, NaH/THF;
(h). Dibal-H, separation isomers and crystallization.

Supplementary Figure 3. Structure of 9-*cis*-β-apo-10´-carotenal. ^{13}C-natural abundance (**1**) and selectively ^{13}C-labeled at position C-11, highlighted in blue (**2***).

Supplementary Figure 4. 1D ^{1}H NMR spectra of 9-*cis*-β-apo-10´-carotenal (I) and (I*). The Spectrum of labelled (**1***) is shown in black and of native (**1**) in red, both in CD_2Cl_2, full spectral range. For experimental details, see Methods section of Supplementary Material.

This article is protected by copyright. All rights reserved.

Accepted Article

Supplementary Figure 5. Expansion of the 1D ^{1}H NMR spectra of 9-*cis*-β-apo-10´-carotenal (1) and (1*). Spectral region 0.8 – 2.3 ppm.

Supplementary Figure 6. Expansion of the 1D ^{1}H NMR spectra of 9-*cis*-β-apo-10´-carotenal (1) and (1*). Spectral region 5.9 – 7.45 ppm.

Supplementary Figure 7. Expansions of the 2D ^{1}H-^{13}C-HSQC spectra (with carbon type editing) of 9-*cis*-β-apo-10´-carotenal (I) and (1*). Compound **(1)** and **(1*)** showing ^{13}C-^{1}H-one-bond ($^{1}J_{CH}$) coupling connectivities between protons and carbons in the corresponding spectral regions. Cross peaks of CH_3 and CH groups appear in blue, cross peaks of CH_2 groups appear in red.

Supplementary Figure 8. **Expansions of the 2D ^{1}H-^{13}C-HSQC spectra (with carbon type editing) of 9-*cis*-β-apo-10´-carotenal (1) and (1*).** For the selectively labelled compound (**I***) 2 intense cross peaks are visible for the ^{13}C*-^{1}H-bond in position C-11, one of which (6.92 ppm/125.9 ppm) showing the same ^{1}H- and ^{13}C- shifts as the 9-*cis* isomer of (**1**) while the other 6.82 ppm / 127.3 ppm indicates the coexistence of the corresponding 9-*trans* isomer of (**1**).

Supplementary Figure 9. Structure of carlactone. ^{13}C-natural abundance (**8**) and with ^{13}C-label recovered at position C-11, highlighted in blue (**8***).

Supplementary Figure 10. 1D ^{1}H NMR spectra of carlactone (8) and (8). The Spectrum of labelled (**8***) is shown in black and of native (**8**) in red, both in CD_2Cl_2, full spectral range. For experimental details, see Methods section of Supplementary Material.

Supplementary Figure 11. Expansion of the 1D ^{1}H NMR spectra of (8) and (8*). Spectral region 0.8-2.1 ppm.

Supplementary Figure 12. Expansion of the 1D ^{1}H NMR spectra of (8) and (8*). Spectral region 5.0 – 7.5 ppm. For (**8***) the resonance of 11-H is split into a doublet due to one-bond coupling of 11-H with the ^{13}C enriched 11-C* ($^{1}J_{CH}$ = 180 Hz). In addition, ^{13}C-enrichment at 11-C leads to long-range coupling interactions with the neighboring 12-CH group. This is evident from the ^{1}H resonance of 12-H, which is a poorly resolved pentet in (**8**) and is further split into a doublet in (**8***) with a coupling constant of $^{2}J_{CH}$ = 7.8 Hz.

Supplementary Figure 13. **Expansions of the 2D ^{1}H-^{13}C-HSQC spectra (with carbon type editing) of carlactone (8)** and **(8*).** For compound (**8***) a cross peak of enhanced intensity is visible for the ^{13}C*-^{1}H-bond in position C-11, while the remaining cross peaks become visible after

This article is protected by copyright. All rights reserved.

increasing the scale by a factor of 64. The ^{1}H-^{13}C-HSQC cross peak of 12-CH at 6.9 ppm/142.7 ppm of (**8**) was not visible in the 2D spectrum of (**8***). This can be explained by a strong signal intensity loss of the 12-CH cross peak during the two delays (adjusted to 1/2 and 1/4 of $^{1}J_{CH}$, respectively, with $^{1}J_{CH}$ = 145 Hz) of the HSQC experiment (with multiplicity editing) due to coupling of the carbon nuclei at 12-C with their adjacent ^{13}C enriched nuclei at C-11. To support this, a simulation of the same HSQC experiment was performed confirming the unwanted impact of C-C coupling between adjacent ^{13}C carbons on the signal intensity of the HSQC cross peaks (**Supplementary Figure 14**).

Supplementary Figure 14. **Simulation of ^{1}H^{13}C-HSQC (*hsqcedetgpsisp2.2*) experiment.** The «NMRsim» software (Bruker) was used for fictitious spin systems of two weakly coupled pairs of nuclei (11-CH, 12-CH) and one isolated (ref-CH) as reference. Overlay of 2D ^{1}H-^{13}C-HSQC spectra with assumed $^{1}J_{CC}$-coupling constants of 0Hz (blue), 45 Hz (pink) and 72.5 Hz (red) slightly shifted to each other. The simulation demonstrates that the signal intensities of the C-H-cross peaks may become strongly reduced due to C-C coupling. Because of the low natural abundance of ^{13}C isotopes (~1.1 %), this C-C coupling is usually negligible in the spectra of unlabeled compounds, but may no longer be neglected with ^{13}C-enriched compounds.

Supplementary Figure 15. 3D-representation of chemical species proposed to be involved in the conversion of 9-*cis*-β-apo-10'-carotenal (1) into carlactone (8). The structures are as presented in Figure 1 (main text) in 2D. The numbering and labeling corresponds to that of Figure 1. The conformations were obtained with the Avogadro software [5] and the energy minimization algorithms included. The colored spheres (green and dark red) represent the molecule parts that are chemically not involved. They have been omitted from the intermediate species, for clarity. The curved arrow in red denotes the rotation around the C12-C13 bond required for converting the *transoid* conformation into the *cisoid* one as depicted in structure (**2**).

Supplementary Figure 16. Inverted reaction sequence. The inverted sequences of oxygenation ((**b**) and (**e**) in Figure 1) and rearrangement steps ((**d**) and (**f**)) would lead to a product lactone (analogous to **8** in Figure 1) linked to a molecule fragment derived from R_2.

This article is protected by copyright. All rights reserved.

Accepted Article

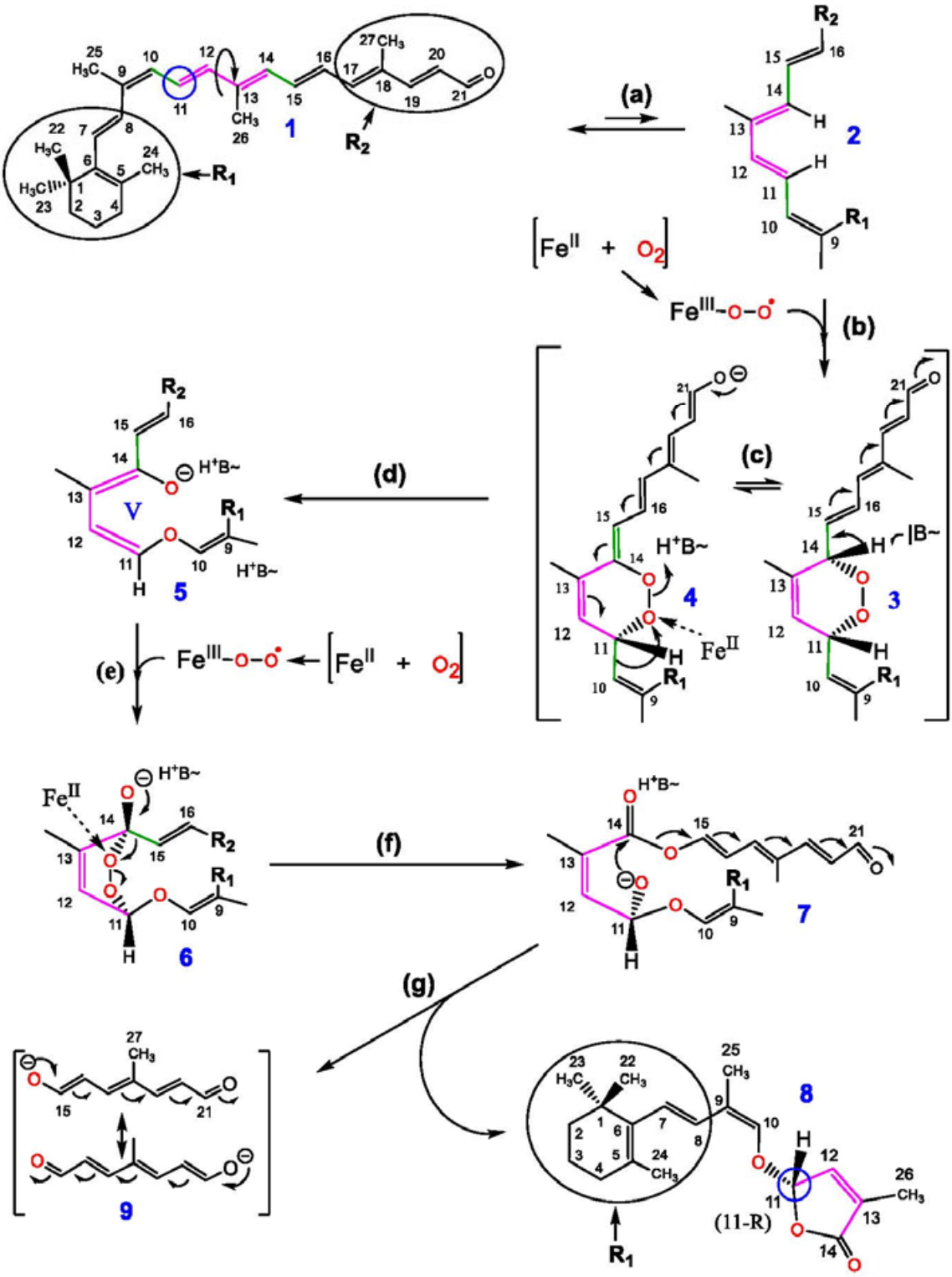

This article is protected by copyright. All rights reserved.

Accepted Article

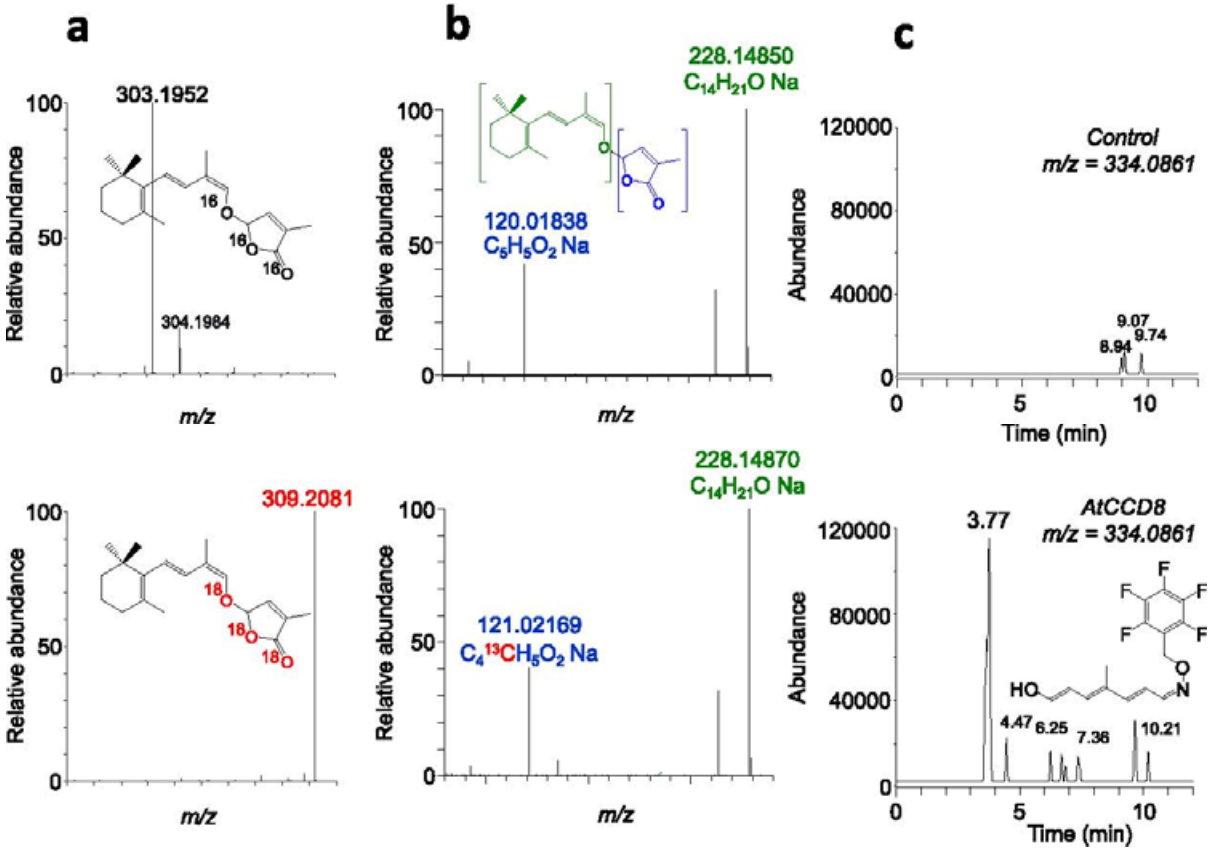

This article is protected by copyright. All rights reserved.

Accepted Article

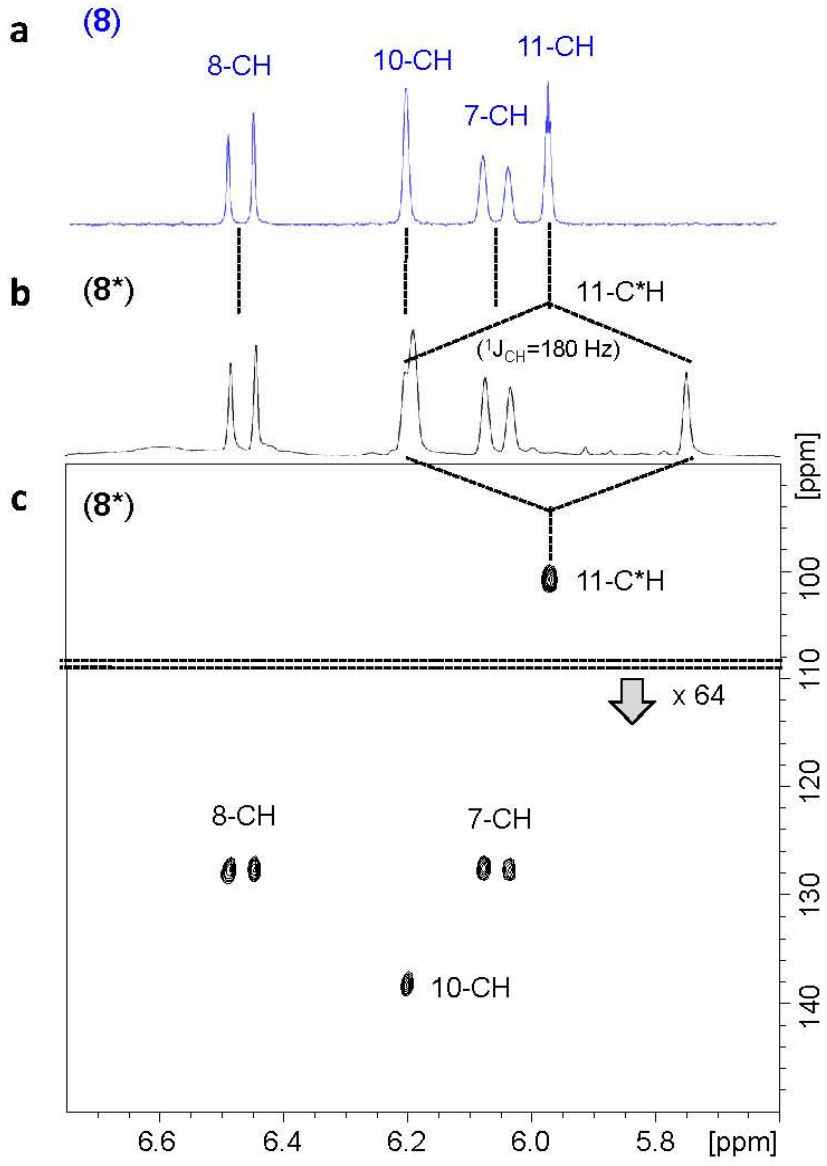

This article is protected by copyright. All rights reserved.